

Radiation effects in optical coatings for ITER diagnostics

A. Pereira^{a,*}, M. Medrano^a, E. Leon-Gutierrez^a, C. Pastor^a, F. Mota^a, R. Vila^a, C. Rodriguez^a, R. Carrasco^a, F. Lapayese^a, A. de la Peña^a, A. Soletto^a, E. Rincón^a, S. Cabrera^a, V. Queral^a, A. Fernández^a, R. López-Heredero^b, C. Torquemada^b, T. Rodrigo^b, L. Gómez^b, T. Belenguer^b, L. Vermeeren^c, W. Leysen^c, J. Piqueras^d, F. Le-Guern^d, C. Alén-Cordero^e

^a CIEMAT - Laboratorio Nacional de Fusión, Avda. Complutense 40., Madrid 28040, Spain

^b INTA - Área de Óptica Espacial, Ctra. Ajalvir km 4 Torrejón de Ardoz, Madrid 28850, Spain

^c SCKCEN - Belgian Nuclear Research Centre, Boeretang 200, Mol 2400, Belgium

^d F4E - Josep Pla 2, Torres Diagonal Litoral B3, Barcelona 08019, Spain

^e UAH - Dep. de Teoría de la Señal y Comunicaciones, Alcalá de Henares 28805, Spain

ARTICLE INFO

Keywords:

Radiation-resistant
Field lens
Optical coating
Parylene-C
Sapphire
YAG
BaF₂

ABSTRACT

The aim is to provide an assessment of radiation damage in coated films on refractive substrates that could be used as relevant information to protect the field lenses in optical diagnostics for ITER. Radiation-resistant optical materials with transparent properties should transfer light from plasma to detectors through the interspace until the port cell area where they are located (more than 10 m from the vacuum window). These optical coatings and substrates should have resilience enough to withstand neutron and gamma irradiation without significant degradation of their transmittance.

Coated sapphire (Al₂O₃ windows), YAG with Broad Band Anti-Reflective (BBAR) and substrates of BaF₂/CaF₂ protected with anti-humidity coating (Parylene-C) were extensively tested. After testing, transmission measurements and analysis of optical surfaces yield significant discoveries. All substrates showed good refractive performance under gamma radiation. On the contrary, Parylene-C did not resist temperatures above 100 degrees Celsius as expected, according to manufacturing specifications. In addition, it was observed that with an energy dose of 332 kGy of gamma rays and a significantly lower temperature of 50 degrees Celsius, the Parylene-C protection is also damaged. Coated sapphire had the best overall performance with respect to the neutron irradiation tests. Nevertheless, the decrease in transmission observed in the YAG and BaF₂ coated samples is not significant for the expected cumulative neutron dose that these samples will receive at their location within the diagnostic.

This information was considered for the selection of the best candidates as refractive lenses and optical coatings for the Preliminary Design Review (PDR) of ex-vessel components that will integrate the Wide-Angle Viewing System (WAVS) for ITER Equatorial Port 12.

1. Introduction

The ITER Equatorial Port Wide Angle Viewing System (WAVS) is an optical diagnostic that will provide real-time measurements of the visible and infrared light coming from the main chamber wall [1]. These measurements will contribute to the safe operation of the machine by providing information about the temperature of the plasma-facing components, preventing any potential damage [2]. The WAVS diagnostic will be present in four Equatorial Ports (EP), #3, #9, #12 and #17. Each EP will have four Lines of Sight (LoS), except for EP #12 (with

3 LoS) which is currently in the final design of the system and the Final Design Review (FDR) scheduled for late 2022. A first conceptual development for the WAVS system was presented at [3]. Preliminary design and analysis of interfaces can be found in [4,5]. The optical designs of the Port-Plug (PP) components, specially mirror elements, were presented in [6]. The ex-vessel optics across the Interspace (IS), Bio-shield (BS) and Port Cell (PC), based also on mirrors and refractive elements, were exposed in [7]. All these optical elements were designed with opto-mechanical modules that can be assembled, integrated and verified as independent sub-systems [8]. Additionally, structural

* Corresponding author.

E-mail address: augusto.pereira@ciemat.es (A. Pereira).

<https://doi.org/10.1016/j.fusengdes.2023.113438>

Received 19 October 2022; Received in revised form 11 December 2022; Accepted 27 December 2022

Available online 13 January 2023

0920-3796/© 2023 Elsevier B.V. All rights reserved.

analysis [9,10] (thermal, electromagnetic and inertial loads) were required to guarantee both the mechanical integrity and the optical performance of the system. Nuclear analysis [11] and shutdown dose rate calculations [12] have also been carried out to complement the support to the design of the IS components.

To address a crucial issue of the optics lifetime due to the very harsh conditions of ITER, extensive research tests were performed on diagnostic mirrors and refractive lenses. It was supported by F4E organization and coordinated between CIEMAT and INTA (Spain), KIT (Germany) and SCK-CEN (Belgium) laboratories. The impact of baking and steam ingress tests on coated first mirrors has already been studied in [13]. This evaluation provided the selection of the best candidates as reflective materials for the PP-EP#12-WAVS diagnostic. Being mainly an optical system, the WAVS will be integrated also by coated lenses, beam splitters and vacuum windows, specifically in the ex-vessel area. These refractive components are even more sensitive to radiation than other metallic and mechanical components. For this reason, it is also relevant to provide an assessment of radiation damage in coated films and transparent substrates which should behave with resilience enough to withstand neutron and gamma irradiation without significant degradation in its transmittance. The results of this work gave support, from the first optical designs until the FDR stage, for the selection of the best candidates as refractive optical materials for the IS, BS and PC areas belonging to the EP#12-WAVS diagnostic.

2. Background

The WAVS will comprise several optical systems transferring the radiation (by means of a broad set of refractive lenses) from the main plasma and plasma-facing components to detectors located in the port cell. In addition, diagnostic windows are part of the primary confinement of ITER [14]. This limit must be fully guaranteed under normal and accidental conditions. Therefore, window assemblies are classified as Security Component Class 1 (SIC-1) and must be available continuously during the useful life of ITER. Consequently, high reliability with good mechanical properties of window assemblies is required and demanded.

On the other hand, radiation-induced effects on coated field lenses and window assemblies (mainly transmission degradation) of various refractive materials such as silicon (Si), fused silica (SiO₂), sapphire (Al₂O₃), spinel (MgAl₂O₄), YAG (Y₃A₅O₁₂ Yttrium-Aluminum Garnet), ZnS, ZnSe, BaF₂, CaF₂, ALON (ALuminum OxyNitride), etc., which are typically protected with transparent thin films as Broad Band Anti Reflective (BBAR) or anti-humidity coatings, have been extensively studied in the past [15–20]. Nevertheless, radiation sensitivity of substrates and coatings should be evaluated with regard to the specific design solutions for the WAVS system. Restrictions in the available space for the ex-vessel optics, led us to discard the use of reflective optics for the optical design. For more than 10 m along the WAVS, most of the lenses must simultaneously transmit in dual band, the visible (VIS) and infrared (IR), in a common optical path that goes from the IS to the Shielded Cabinet (SC) in the PC area. However, the index of refraction of optical materials for the different wavelengths is different, and consequently a different response and correction of the aberrations is inherently present. The main consequence that arises from this is the chromatic aberration. Additionally, the number of materials transparent common to both bands is also limited and therefore the choice of optical materials offers us less degrees of freedom for the design of the optics. This limited choice of materials greatly conditions the optical correction. Furthermore, optics must withstand severe environmental conditions at different radiation levels. To obtain a range of appropriate window materials and coated field lenses suitable for the WAVS radiation environment, an extensive R&D program including testing and measurements was performed.

Due to the above design constraints, many commonly used refractive substrates as silicon and fused silica were not included on experiments. Although there is a wide variety of them, they have worse mechanical

strength than sapphire and a higher radiation-induced transmission degradation [21]. Regarding the ceramic transparent materials as ALON and spinel, both exhibit good broadband transmittance from VIS to mid-IR but for our experiments were not tested with neutrons. Instead, the ceramic-polycrystalline YAG seems to have excellent high-temperature mechanical properties and a greater corrosion resistance [22]. Other transparent materials as BaF₂ and CaF₂ have completed the list of tested substrates. Concerning ZnS, ZnSe optical substrates, both are not candidates for use near the Vacuum Window (VW), even though they are the most widely used IR transmitting window materials [23]. Results of irradiation for ZnS were already studied in [24]. This investigation resulted in significant transmission degradation due to displacement effects.

From an optical point of view, an anti-reflective coating is one or more thin layers of material deposited on an optical substrate which alters the way the optic transmits light by reducing spurious reflections from surfaces. BBAR protection improves the transmission efficiency of lenses, beam splitters or windows and expands contrast by reducing the stray light. Thin-film coatings are also required to operate and survive in environments that include high humidity as it is the case of the ex-vessel rooms of the WAVS system. When considering irradiation on field lens coatings, the most likely deteriorating effects are, the change of the refractive index of materials, the thickness drop of the layers and specially, the transmission degradation. In general, the number of works in which the effects of neutron and gamma irradiation on the optical properties of anti-humidity coatings were studied is limited. For instance, not enough scientific articles dedicated to the study of anti-humidity coating Parylene-C were found. In this line and after the neutronic and gamma tests performed with this coating, transmission measurements and the analysis of the optical surface of Parylene-C yield significant discoveries fully explained below on the current research.

3. Experimental procedure

All experimental WAVS samples had a diameter of $\varnothing 12 \pm 0.2$ mm and 2 ± 0.1 mm of thickness, roughness minor than 10 nm of root mean square (RMS). A thickness from 2 to 14 μ m was used as standard value for the coatings.

In optical coatings, thermal testing can induce significant damages (cracks, delamination, etc.). For this reason, it is important to validate the resistance of coatings to high temperatures. To check whether additional verifications could complement the validations achieved by gamma and neutron irradiation, thermal tests were also implemented on specific samples, following ex-vessel conditions. The climatic chamber to accomplish the thermal tests at a low temperature (to check the temperature at ITER operation within the IS) was provided by INTA (Spain). A set of samples were submitted to 55 °C and a relative humidity of 95% during 16 h in a Heraeus HCT030 N/S 44902 Climatic Chamber. The climatic chamber to carry out the thermal tests at a higher temperatures (to check the baking condition foreseen at ITER) was provided by CIEMAT (Spain). The window samples were submitted to 240 °C in air through 60 days by means of a muffle furnace Therm-concept KM07/12/M and a Yokogawa SR10003 data acquisition recorder. The working spectral range for experiments covers the VIS spectrum (400 – 700 nm) and two IR wavelengths (3 and 5 μ m). In order to determine the test impact on the samples (about thermal and gamma irradiation conditions), the following measurements were performed before and after test:

- Transmission over the IR and VIS spectral bands (measurement uncertainty below 2% for both ranges). VIS spectrometers used are models Varian Cary 5E and Perkin Elmer Lambda 950. Infrared spectrometers models, Nicolet 5700 FT-IR and Perkin Elmer GX
- Wavefront error (WFE) to evaluate the surface quality. A Fizeau ZYGO interferometer and the MetroPro® program were used to measure and analyze the WFE

- Surface analysis through of Secondary-Ion Mass Spectrometry (SIMS). Model SIMS/SNMS Workstation of Hiden SIMS Foundation company.
- Adherence (for coated samples, after finished the measurements)

In accordance with the neutronic assessment [11], the gamma flux expected at the position of VW will be $7.24E+08 \text{ pcm}^{-2}\text{s}^{-1}$ and the neutron flux $1.00E+09 \text{ ncm}^{-2}\text{s}^{-1}$ which corresponds to a gamma dose of $1.22E+16 \text{ pcm}^{-2}$ and neutron dose of $1.69E+16 \text{ ncm}^{-2}$ respectively, according to the 4700 h of total expected life of ITER working with neutrons [25]. Therefore, the absorbed energy dose to be performed on sample's materials was 272 kGy, taking into account the sapphire as feasible reference for the VW (332 kGy including an additional safety value).

The optical characterization of refractive materials and coatings with the gamma radiation test was carried out at Nayade/CIEMAT facility (Spain), with a ^{60}Co radioactive source and a constant dose rate of 5,04 kGy/h. All samples were irradiated with a total radiation dose of the previously mentioned by the computational model with an addition of a safety factor given a total value of 332 kGy, equivalent to 2,75 days of irradiation time in Nayade. Cumulative doses of 564 kGy (4,67 days) and 1370 kGy (11,34 days) were also carried out to check if the most resistant samples previously tested would resist additional dose.

Finally, regarding the neutron test, WAVS lenses were irradiated and measured in BR1/SCKCEN facility (Belgium). The irradiation time should aim targeting an equivalent damage at 14.1 MeV corresponding to the ITER fluence of about $1,7 \times 10^{16} \text{ ncm}^{-2}$. This would lead to a required irradiation time of 240 h or 35 full days. In order to determine a trend in the sample degradation 4 irradiation steps were defined: about 3 h (1% of the total radiation time), 3 additional days (10%), 14 additional days (50%) and 18 additional days (100%). Before the start of the irradiation and after each irradiation step transmission measurements of all windows were performed. The spectrometer used for the transmission measurements was a Perkin Elmer Lambda 1050 with an operating window of 200–3300 nm.

4. Analysis of transmission before and after tests

Table I shows the list of anti-reflective materials and refractive samples with information about transmission after tests, WFE measurements and adherence test. Degradation on transmittance is considered when there is a deterioration of at least 15% between measurements before and after test. On the other hand, unaffected categorization denotes the best results with no changes on transmittance and/or WFE behavior. The WFE results show the difference between the RMS values of roughness prior and after test (in absolute values). Values greater than 30 nm in ΔRMS can be considered as an appreciable

deterioration of the surface quality in terms of wavefront distortion. If the overall optical quality of one sample does not meet with the supplier specifications, i.e., samples that do not fulfill the specification required (Peak to Valley value, $\text{PV} > 1\lambda$ at 633 nm), the WFE is also evaluated as 'Affected'.

Coated and uncoated samples were tested with the same substrate composition in order to compare its behavior between them. Sapphire and YAG with BBAR reached the best overall performance in terms of refractive transmission. On the opposite side, the Parylene-C optical coating have got the worst results. Alon and spinel did not perform too well, even at the lowest exposure dose of 326 kGy. Zinc substrates (sulfides and selenides) with BBAR did not experience large deteriorations in their transmittance, but from the beginning, the absolute pre-measurement values were not high enough. In addition, in some of these samples, a loss of surface quality verified with the WFE measurement, was found. For this reason, neither of them has been tested with neutrons. Optical samples irradiated with both, gammas and neutrons are highlighted in gray color. A special case was the combination of CaF_2 and BaF_2 with the Parylene-C. Despite the fact that this coating has failed in all the tests, very relevant information has been obtained from the study of the behavior of this material in relation to its temperature and the irradiation test carried out. Before explaining this information in detail, next are represented some graphs reflecting the data previously exposed within the Table I.

Showing the most affected materials first, in Fig. 1 and on the Alon

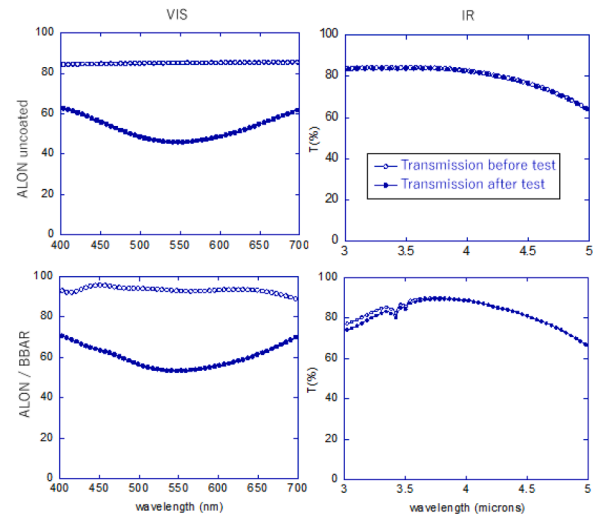


Fig. 1. Transmission of uncoated and coated Alon lenses.

Table I

List of tested samples.

Substrate	Coating	Gamma irradiation test			WFE	Adherence	Neutronic test			
		Transmission at (gamma dose/days):					Ranking by Transmission at			
		332 kGy	564 KGy	1370 KGy			500 nm		3300 nm	
		2,75 days	4,67 days	11,34 days						
Sapphire	BBAR	Not affected			Not affected	Not affected	1	82,10%	1	95,70%
ZnS	-	Not affected			Not affected	Not affected				
ZnS	BBAR	Not affected	Not affected	Not affected	Affected	Affected				
ZnSe	-	Not affected			Not affected	Not affected				
ZnSe	BBAR	Not affected	Not affected	Not affected	Affected	Not affected				
YAG	-	Not affected			Not affected	Not affected				
YAG	BBAR	Not affected	Not affected	Not affected	Not affected	Not affected	2	74,00%	2	95,30%
Alon	-	Affected			Affected	Not affected				
Alon	BBAR	Affected			Not affected	Not affected				
Spinel	-	Affected			Not affected	Not affected				
Spinel	BBAR	Affected			Affected	Affected				
CaF2	Parylene-C	Affected			Not affected	Not affected				
BaF2	Parylene-C	Affected	Affected	Affected	Affected	Not affected	3	54,50%	3	88,60%

samples, in the VIS range is checked a significant degradation after test due to substrate degradation. Instead, in IR range no variation of transmittance was observed. For the BBAR coated sample and in the same way, important degradation of visible transmittance appears after test. In IR range small variation of transmittance is observed. Weak absorption bands were detected at 3.4 and 3.5 μm .

Significant decrease of transmittance of coated spinel is perceived after 332 kGy of gamma irradiation. In IR range, a light increase of transmission of Spinel is observed after test. Weak absorption bands were also observed at 3.4 and 3.5 μm .

A similar behavior has got the uncoated spinel sample at VIS wavelengths (Fig. 2).

Although apparently the combination ZnS/BBAR did not exhibit losses in its transmission as shown in Fig. 3, WFE and the adherence test detected deterioration and delamination on its coated optical surface.

Concerning the ZnSe substrate protected with BBAR (Fig. 4) the VIS transmittance is quite low when compared with the ZnS sample (Fig. 3). Instead, the good behavior of these lenses in the IR zone is fulfilled.

In the following section, a significant performance of Parylene-C is characterized by the joint combination of a specific temperature and an irradiation dose.

5. BaF₂/Parylene-C behavior after tests

Parylene-C is a crystalline polymer which results in generally high mechanical strength with just an ultra-thin coating that can start at 0.5 μm thick. It is also an exceptional moisture and chemical protection. The anti-humidity coating seems to maintain its integrity under 110 °C (recommended by many manufacturers) and it is lost above higher temperatures in the presence of non-inert environments [26].

This behavior was verified by testing two thermal experiments in air (atmospheric pressure) by means of two different optical samples with the same composition (BaF₂ with Parylene-C) as it is shown in Fig. 5. On the right graph, transmittance improves after tests due to degradation of Parylene-C layer. This is an anomalous behavior when a layer has disappeared. Between 200 and 350 of wavelength spectral bands a clear pattern is reproduced. Good coating performance is also shown in the graph on the left. Coating deterioration was also confirmed by using a surface analysis technique by means of the SIMS spectrometry applied to the previous BaF₂/Parylene-C samples (Fig. 6). SIMS can obtain compositional data down to the count per second (cps) range and is compatible with any material that can reliably be tested from depths of several hundred nanometers (nm) to a single atomic layer.

The figure above (top graph) shows that the most common material

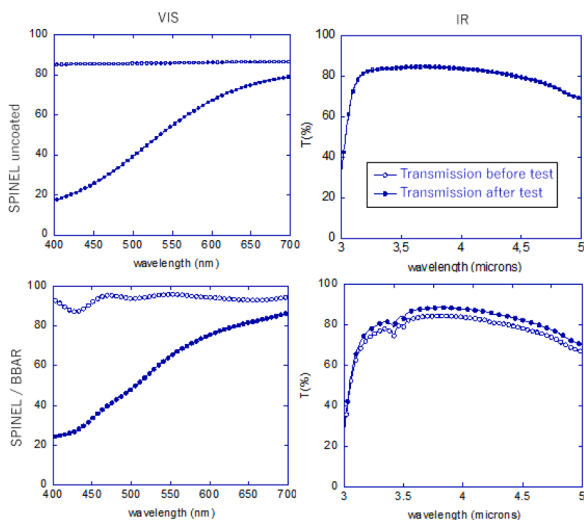


Fig. 2. Transmission of uncoated and coated spinel lenses.

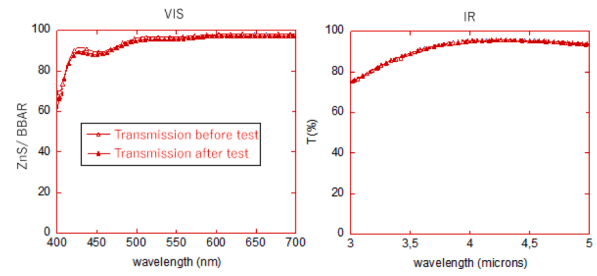


Fig. 3. Transmission of ZnS lens protected with BBAR.

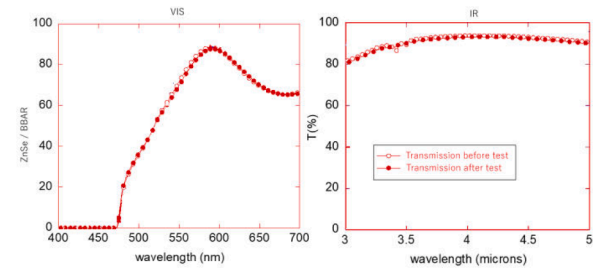


Fig. 4. Transmission of ZnSe lens protected with BBAR.

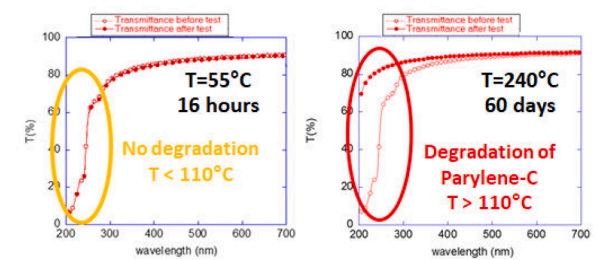


Fig. 5. Thermal test on BaF₂/Parylene-C samples.

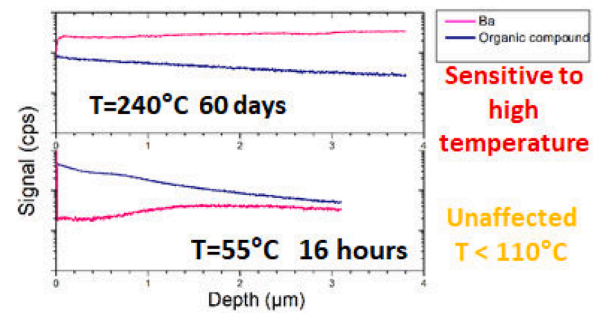


Fig. 6. Assessment with the SIMS technique after thermal tests.

on the surface is the element Barium. This confirms that the coating has been deteriorated due to excess of temperature (240 °C). Nevertheless, in bottom graph Barium has been protected with the Parylene-C coating in its surface since temperature did not exceed the limit of 110 °C and the most common material found on the surface was a polymer.

When other similar samples were analyzed with the gamma radiation at a dose of 332 kGy and below the temperature limit of 110 °C, the pattern of behavior in lens transmission was repeated, with wavelengths appearing where the transmittance was lower before the gamma test.

The transmission pattern was more remarked as the radiation dose was increased while maintaining the same temperature of 50 °C (Fig. 7). BaF₂ improves transmittance due to degradation of Parylene-C coating. Same behavior as thermal test above 110 °C. In the same way, SIMS also

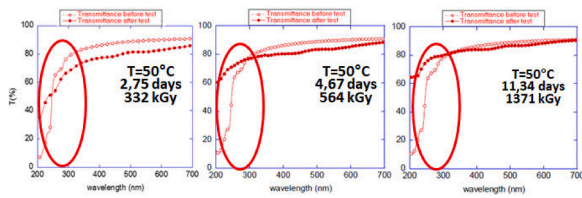


Fig. 7. Gamma radiation test on BaF₂/Parylene-C samples.

confirmed the material analysis on its surface (Fig. 8), barium as predominant element above the lens surface, as expected.

Despite having already been characterized the BaF₂/Parylene-C optical samples with the gamma irradiation and exposing its increase of transmittance by means of losing the protected layer due to the joint combination of the gamma dose and a low temperature, anti-humidity protected BaF₂ samples were again tested with a neutronic irradiation dose.

After performing BaF₂/Parylene-C samples with a neutron dose of $1.7 \times 10^{16} \text{ n/cm}^2$, the next evaluation can be done. Transmission increases in UV range (200–300 nm) after the first irradiations and coating begins to deteriorate as the behavior pattern in transmission behaves as in the thermal and gamma test. Instead, at the total dose (100% of neutron dose), transmission decreases as BaF₂ was affected by neutrons (arising a diffuse layer with spots). The loss is also confirmed in the range of 600–700 nm. But in this case affecting to the substrate. Finally, some activation at 50% has been measured and the coating irreversibly detached from its optical surface (see Fig. 9)

6. Sapphire and YAG lenses with BBAR

YAG with BBAR were not influenced by gamma radiation even with 1371 kGy (around 500% higher with respect to the nominal dose). Similar transmittance before and after test is observed on Fig. 10.

Sapphire window with BBAR had the overall best performance with the neutronic irradiation (Fig. 11). Both materials YAG and Sapphire showed some activation at 50% of irradiation.

Near UV range, transmission decreases gradually after the first stages of irradiation. In the VIS range, the loss of transmission is quite low. BBAR coating was not detached.

7. Assessing the damage on the first set of lenses

Fig. 12 shows a schematic view of the three LoS of the EP#12-WAVS showing the current position of the three first doublets closest to the VW that is located at the end of the optical hinge..

As observed, the shortest distance comparing the three LoS belongs

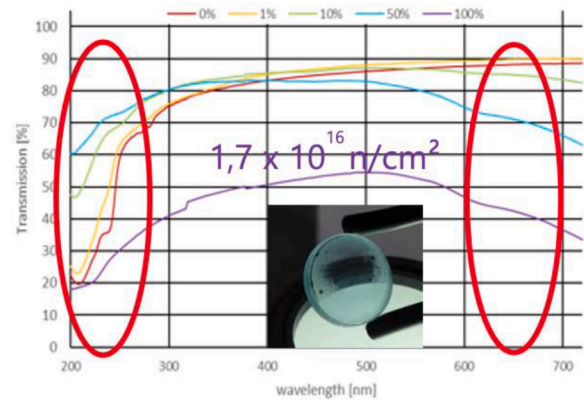


Fig. 9. Transmission on BaF₂/Parylene-C after neutron test.

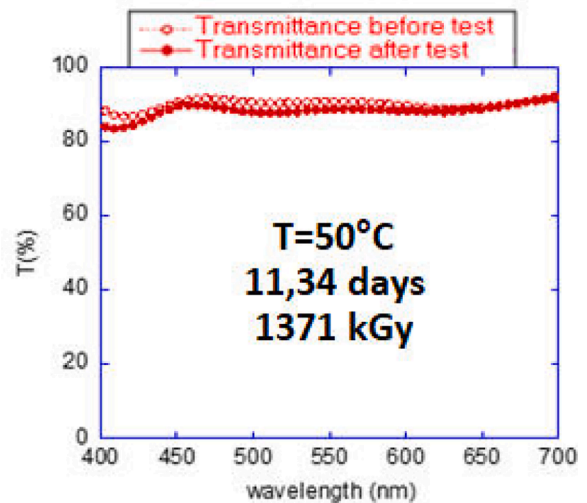


Fig. 10. Transmission of YAG/BBAR after gamma test.

to the Divertor one (bottom LoS). The separation between the VW and this first doublet of the Divertor LoS is approximately 1800 mm

So far, current optical design (at FDR level) is using sapphire and CaF₂ as substrates for the first set of lenses closest to the VW, both with BBAR protection as representative composition. Using this setup, the optical engineers obtain better performances regarding the optical parameters and meet expectations regarding the present tests exposed in the current work. But, to assess the damage to the first set of lenses, it would be significant to know how much radiation they will receive. At the bottom of the Fig. 12 is clearly indicated, field lenses were tested with a final neutron flux of near $2E10 \text{ ncm}^{-2}\text{s}^{-1}$, this value is bit greater than the expected calculation value used as a reference acquired by means of the neutronic model (obtained by using MCNP5 v1.6 code) for this position at the VW. From the model, the foreseen fluence rate and expected dose exactly at the position of the two identical doublets located in the Divertor LoS is shown also in the Fig. 12, i.e., fluxes of $1.55E8 \text{ ncm}^{-2}\text{s}^{-1}$ and doses of $2.62E15 \text{ ncm}^{-2}$. Those quantities are clearly lower than the experimented with the neutronic test. Fluxes are an order of magnitude smaller (exactly ten raised to eight which is below than ten raised to nine) and the total dose is also below one order of magnitude smaller (power of fifteen instead of the power of sixteen carried out with neutrons).

Fluxes and doses of neutrons expected on the two set of lenses are quite low, 15% and 11% respectively regarding the total dose performed with neutrons.

Having a look again to the graphs in Fig. 9, is observed that the decay

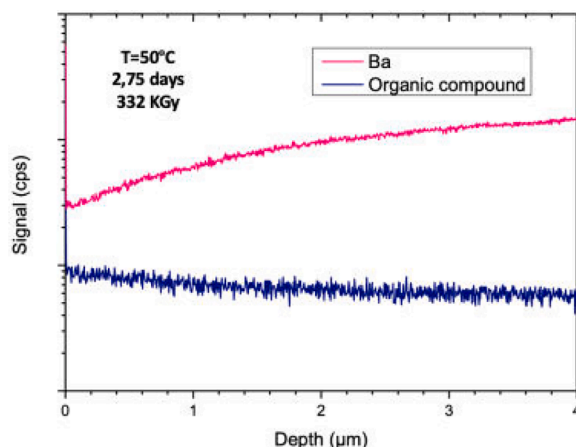


Fig. 8. Assessment with the SIMS technique after gamma test.

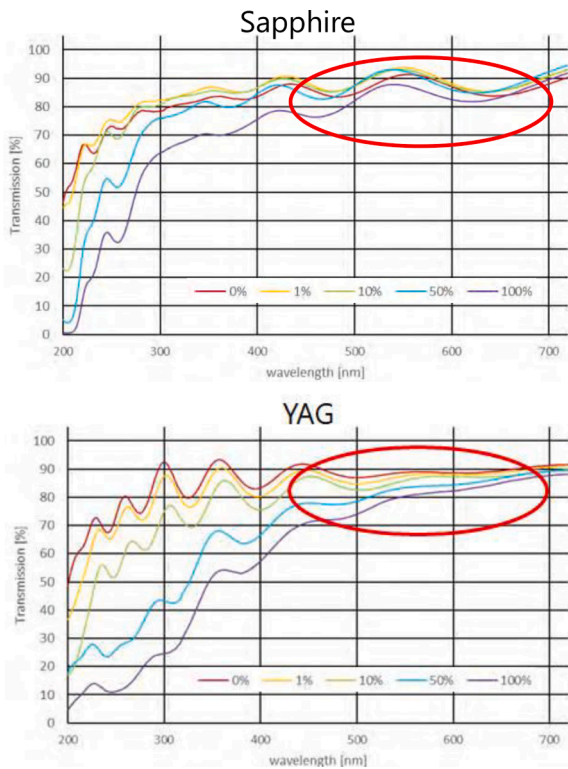


Fig. 11. Transmission on Sapphire and YAG after neutron test.

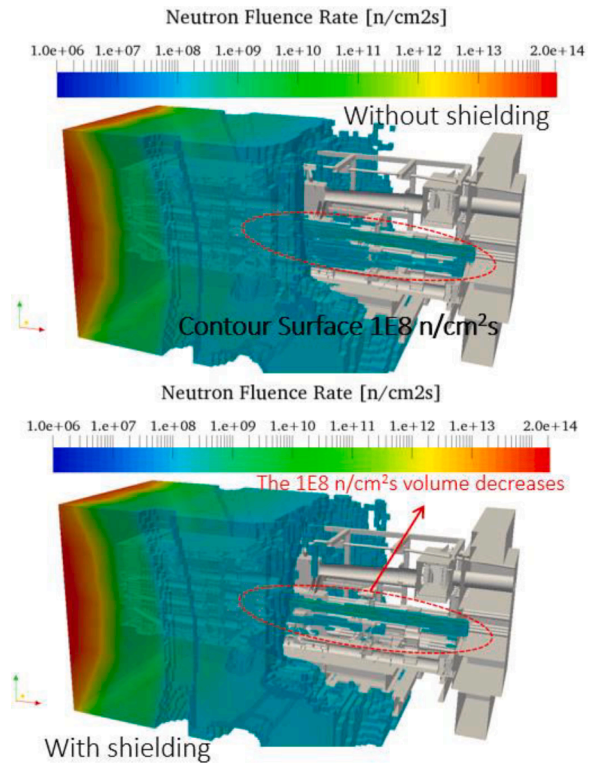


Fig. 13. Neutron Fluence Rate with values close to $1E8 \text{ ncm}^{-2}\text{s}^{-1}$ on the first set of lenses near the VW. The calculations were developed using MCNP5 v1.6 code.

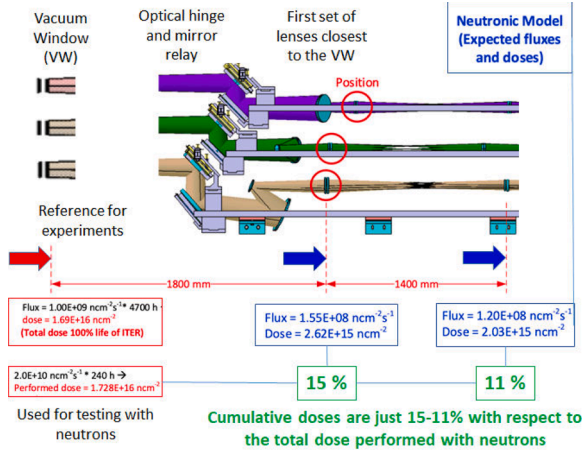


Fig. 12. Cumulative dose on the first set of lenses near the VW.

of transmission at 600 nm for the BaF_2 sample (as the sample with the worst behavior with neutrons) is quite low, just 5%, considering the signal in green color (10% of the total radiation time as the most representative curve close to 15%). It is quite acceptable a loss of transmission of only 5% as the most adverse value degradation for the first refractive optics closest to the VW. At 600 nm with the sapphire and YAG lenses, the loss is neglectable and even less than BaF_2 sample.

Moreover, the previous particle transport calculations were performed without considering any shielding and protection. In Fig. 13, there are two images belong to the former neutronic model on a previous conceptual design that it does not correspond with the current EP#12-WAVS design but, it is very significant to observe the neutron fluence rate contour surface of $1E8 \text{ ncm}^{-2}\text{s}^{-1}$ by comparison between without shielding and with shielding inside the interspace. In the top image it is clearly seen the dominance of the green color. Instead in the bottom image it can be observed as the fluency rate corresponding with the

green color decreases quite a bit. Consequently, the tests were performed with an additional safety value which implies that the final dose used in the tests (332 kGy vs 272 kGy) was slightly overestimated.

8. Conclusions

Parylene-C can be used up to 110°C but with gammas at 332 kGy and a lower temperature of 50°C , the optical coating is damaged too. Parylene-C is not suitable with neutrons. The combination $\text{BaF}_2/\text{Parylene-C}$ did not pass the full set of tests and will not be used for WAVS.

BBAR protection had good results with gammas and appears to be compatible with neutrons from VIS wavelengths (not detached).

In the following ranking order... sapphire and YAG are the best candidates for the WAVS diagnostic. These can be used as perfectly valid transparent substrates against radiation since the first set of lenses will only receive 15% of the total expected dose without degradation of their transmittance.

Declaration of Competing Interest

The authors declare that they have no known competing financial interests or personal relationships that could have appeared to influence the work reported in this paper.

Data availability

Data will be made available on request.

Acknowledgment

The work leading to this publication has been funded by Fusion for Energy under specific grants F4E-GRT-1146 and F4E-407-SG07. This

publication reflects the views only of the author, and Fusion for Energy cannot be held responsible for any use which may be made of the information contained therein.

References

- [1] S. Salasca, et al., Development of equatorial visible/infrared Wide Angle Viewing System and radial neutron camera for ITER, *Fusion Eng. Des.* 84 (2009) 1689–1696, <https://doi.org/10.1016/j.fusengdes.2008.12.088>.
- [2] S. Salasca, et al., Recent technical advancements of the ITER equatorial visible/InfraRed diagnostic, *Fusion Eng. Des.* 86 (2011) 1217–1221, <https://doi.org/10.1016/j.fusengdes.2011.02.015>.
- [3] R. Reichle, et al., Concept development for the ITER equatorial port visible/infrared Wide Angle Viewing System, *Rev. Sci. Instrum.* 83 (10) (2012), <https://doi.org/10.1063/1.4734487>. Vol.
- [4] S. Salasca, et al., The ITER equatorial visible/infra-red Wide Angle Viewing System: status of design and R&D, *Fusion Eng. Des.* (2015) 932–937, <https://doi.org/10.1016/j.fusengdes.2015.02.062>, 96–97.
- [5] L. Letellier, et al., System level design of the ITER equatorial visible/infrared Wide Angle Viewing System, *Fusion Eng. Des.* 123 (2017) 650–653, <https://doi.org/10.1016/j.fusengdes.2017.06.005>.
- [6] S. Vives, et al., Overview of optical designs of the port-plug components for the ITER Equatorial Wide Angle Viewing System (WAVS), *Fusion Eng. Des.* (2019), <https://doi.org/10.1016/j.fusengdes.2019.04.014>.
- [7] C. Pastor, et al., Optical design of ex vessel components for the Wide Angle Viewing System diagnostic for ITER, *Fusion Eng. Des.* 168 (2021), 112607, <https://doi.org/10.1016/j.fusengdes.2021.112607>.
- [8] M. Medrano, et al., Design overview of ex vessel components for the Wide Angle Viewing System diagnostic for ITER Equatorial Port 12", *Fusion Eng. Des.* 168 (2021), 112651 <https://doi.org/10.1016/j.fusengdes.2021.112651>.
- [9] S. Cabrera, et al., Structural analysis of the optical hinge preliminary design for the ITER Wide Angle Viewing System diagnostic, *Nucl. Mater. Energy* 30 (2022), 101134, <https://doi.org/10.1016/j.nme.2022.101134>.
- [10] E. Rincón, et al., Structural analysis of the interspace afocal module of the Wide Angle Viewing System diagnostic for ITER, *Nucl. Mater. Energy* 30 (2022), 101127, <https://doi.org/10.1016/j.nme.2022.101127>.
- [11] I. Palermo, et al., Preliminary neutronic assessments for the development of the VIS/IR diagnostic systems located in the ITER EPP, *Fusion Eng. Des.* 100 (2015) 629–637, <https://doi.org/10.1016/j.fusengdes.2015.08.014>.
- [12] F. Mota, et al., Shutdown dose rate assessment of the interspace components of Wide Angle Viewing System diagnostic for ITER, *Fusion Eng. Des.* 172 (2021), 112916, <https://doi.org/10.1016/j.fusengdes.2021.112916>.
- [13] A. Pereira, et al., Steam-resistant optical materials for use in diagnostic mirrors for ITER, *IEEE Trans. Plasma Sci.* 48 (2020) 6, <https://doi.org/10.1016/TPS.2020.2967460>.
- [14] G. Vayakis, et al., Generic diagnostic issues for a burning plasma experiment, *Fusion Sci. Technol.* 53 (2008) 2, <https://doi.org/10.13182/FST08-A1684>.
- [15] D. Ehr, et al., Radiation effects in glasses, in: *Nuclear Instruments and Methods in Physics Research Section B: Beam Interactions with Materials and Atoms*, 65, 1992, pp. 1–4, [https://doi.org/10.1016/0168-583X\(92\)95006-D](https://doi.org/10.1016/0168-583X(92)95006-D).
- [16] I.I. Orolvskiy, et al., Gamma irradiation of flint glasses for optics in ITER, *Fusion Eng. Des.* 170 (2021), 112525, <https://doi.org/10.1016/j.fusengdes.2021.112525>.
- [17] D. Sporea et al., "Radiation Effects in Optical Materials and Photonic Devices". (2016), 416, ISBN: 978-953-51-2418-4, DOI: 10.5772/61498.
- [18] K.Y. Vukolov, Radiation effects in window materials for ITER diagnostics, *Fusion Eng. Des.* 84 (7–11) (2009) 1961–1963, <https://doi.org/10.1016/j.fusengdes.2009.01.056>.
- [19] J.B. Fortin, et al., Ultraviolet radiation induced degradation of poly-para-xylylene (parylene) thin films, *Thin Solid Films* 397 (1–2) (2001) 223–228, [https://doi.org/10.1016/S0040-6090\(01\)01355-4](https://doi.org/10.1016/S0040-6090(01)01355-4).
- [20] M. J.Herman, et al., Determination of chemical decay mechanisms of Parylene-C during X-ray irradiation using two-dimensional correlation FTIR, *Polym. Degrad. Stab.* 171 (2020), 109024, <https://doi.org/10.1016/j.polymdegradstab.2019.109024>.
- [21] A.K. Islamov, et al., Radiation-optical characteristics of quartz glass and sapphire, *J. Nucl. Mater.* 362 (2–3) (2007) 222–226.
- [22] H. Nozawa, et al., Mechanical properties of fully dense yttrium aluminum garnet (YAG) ceramics, *J. Ceram. Soc. Jpn.* 116 (2008) 649–652.
- [23] D.C. Harris, et al., Thermal, structural, and optical properties of Cleartran® multispectral zinc sulfide, *Opt. Eng.* 47 (11) (2008), 114001–114001-15.
- [24] F.J. Bryant, et al., The effect of zinc displacement on the luminescence of zinc sulphide, *Solid State Commun.* 10 (6) (1972) 501–504, [https://doi.org/10.1016/0038-1098\(72\)90053-1](https://doi.org/10.1016/0038-1098(72)90053-1). Vol.15 March.
- [25] T. Sugie, et al., Spectroscopic diagnostics for ITER, *J. Plasma Fusion Res.* (2003) 10, <https://doi.org/10.1585/jspf.79.1051>.
- [26] M. Yamada, et al., Thermophysical properties of the parylene C dimer under vacuum, *Jpn. J. Appl. Phys.* 59 (2020) 10, <https://doi.org/10.7567/1347-4065/ab5919>. SDDA15.